Cell. Mol. Biol. (ISSN: 1165-158X)

Journal Homepage: www.cellmolbiol.org

Cellular and Molecular Biology

Original Article

Linggui Zhugan decoction as a potential medicine for neuroprotection in Alzheimer's disease via AMPK pathway

Yun Fan[1], Yun Ling[1], Jiulve Hu[2], Zijun Hou[2], Runpeng Dou[3], Chunxiang Zhou[1,*]

[1] School of Traditional Chinese Medicine, Nanjing University of Traditional Chinese Medicine, Nanjing, Jiangsu 210046, China
[2] Zhang Zhongjing Key Laboratory of Prescriptions and Immunomodulation, Zhang Zhongjing Traditional Chinese Medicine College, Nanyang Institute of Technology, Nanyang, Henan 473306, China
[3]Department of Endocrinology, Nanyang Central Hospital, Nanyang, Henan 473005, China

Article Info

Article history:

Received: April 05, 2024
Accepted: May 15, 2024
Published: July 31, 2024

Use your device to scan and read the article online

Abstract

Alzheimer's disease (AD) is a degenerative dementia illness that causes atrophy of the temporal and frontal lobes of the cerebral cortex. Linggui Zhugan (LGZG), a classic Chinese herbal formula, was initially recognized as a safe and effective treatment of cardiovascular diseases for long history. This study intended to assess the effects and the molecular mechanism of LGZG on AD progress. C57BL/6 mice were divided into six groups: normal mice, amyloid precursor protein/presenilin 1 (APP/PS1) mice (model group), positive control group (model mice treated with donepezil), high, medium and low LGZG group (model mice treated with 7g/kg/d, 3.5g/kg/d or 1.75g/kg/d LGZG respectively). Water maze results showed that the escape latency and path length of high and medium LGZG groups declined compared to the model mice, the decline degree was dose-dependent. The hippocampal slices of six groups were analyzed by Nissl-staining, Perls' iron staining and immunofluorescence assay. The results indicated LGZG could restore morphological anomalies and alleviate iron deposition of AD mice, and the GXP4 positive cells increased significantly. The MDA, Fe2+ and GSH were measured by biochemical testing, whose results illustrated that LGZG could normalize MDA, Fe2+ and GSH levels in AD model compared to un-treated APP/PS1 model. The higher dose of LGZG the mice received, the more intensive effects on those levels of molecules. Western blot results showed that LGZG could affect NeuN, AMPK, p53, SLC7A11 and GPX4 levels in the hippocampus of AD model, which was all proteins related to AMPK pathway. In conclusion, LGZG has a neuroprotective effect on AD through AMPK pathway by alleviating oxidative stress and ferroptosis.

Keywords: Alzheimer's disease, AMPK pathway, Ferroptosis, Linggui Zhugan decoction, Neuroprotection, Oxidative stress.

1. Introduction

Patients with Alzheimer's disease (AD), also known as Senile's Dementia (SD), mainly exhibit an unexpected and irreversible progressive neurodegenerative behavior. Alzheimer's disease typically deteriorates cognitive function and self-care ability of older individuals (aged≥65 years) with age [1]. It is not surprising that the public health burden that comes from Alzheimer's disease is heavy and un-solved issue worldwide. To date, for women patients with Aβ plaque accumulation, lifetime risk of AD and cognitive impairment has been estimated to be 41.9%, while for men is 33.6% [2], forecasting a bleak picture of the future. Recently, the incidence and prevalence rate of AD combined with severe AD rates have kept rising. AD is treacherous in its early stage because of the complexity of the brain and the misdeeming for normal functional degeneration [3], this concealing feature causes delayed AD diagnosis until the serious stage. To date, there is no established standard therapy for AD. Therefore, focusing on the molecular mechanisms of AD progress and searching for new treatment strategies will improve the survival quality of patients with AD.

Linggui Zhugan decoction (LGZG), decocted with four Chinese medical herbs: Ramulus Cinnamomi (Gui zhi), Poria cocos (Fu Ling), white atractylodes rhizome (Bai shu), and Radix Glycyrrhizae (Gan cao) at the ratio of 3:4:3:2 (w/w/w/w), initially recognized as a safe and effective treatment of cardiovascular diseases with a long history in China [4]. Increasing evidences show that LGZG has the potential to treat hyperlipidemia [5], non-alcoholic fatty liver disease [6] and slow down the cognitive decline [7].

LGZG was reported to exert therapeutic effects via AMP-activated protein kinases (AMPK) pathways [8]. AMPK signaling widely demonstrated to be vital for tackling aging based on the important role of AMPK signaling for energy sensors, autophagy and mitophagy [9]. AMPK is a well-known nutrient regulator of brain physiology and homeostasis in cognitive interventions [10]. Furthermore, it has been revealed to facilitate to prevent

* Corresponding author.
E-mail address: chunxiangzhou@njucm.edu.cn (C. Zhou).
Doi: http://dx.doi.org/10.14715/cmb/2024.70.7.23

pathogenic age-related deterioration by neurotransmitters and neurotrophin signals such as paraquat.

To date, the effect of LGZG in Alzheimer's disease via AMPK pathway is still under debate. We aimed to investigate if LGZG contributes to alleviating neurotic atrophy caused by Alzheimer's disease and its treatment mechanism. We hypothesized that LGZG can exert neuro-protection on dementia. This study may offer a novel therapeutic strategy for AD.

2. Materials and methods

2.1. Pathway and functional enrichment analysis

Single-sample gene set enrichment analysis (ssGSEA) algorithm was conducted to forecast the relationship between AMPK pathway and AD. The algorithm identifies the pathway related to AD drug target MAPK3 and the AMPK-related genes that are under MAPK3 pathway regulation.

2.2. AD model modeling and treatment

APP/PS1 mice were generated by Swedish (N595L/K594M) mutation and knockdown PS1 gene in exon 9 to accumulate Aβ plaques in brain. Since APP/PS1 abnormality triggered more obvious cognitive deficits in female and elderly mice, 6 months and weighed 200±20 g APP/PS1 mice (female, C57BL/6; Jackson Laboratory) and age-matched wild-type mice (female, C57BL/6; Jackson Laboratory) as controls were bred with a standard diet in SPF environment.

Mice were randomly divided into six groups (6 mice per group): normal group (wild-type mice, normal saline), model group (APP/PS1 mice received normal saline), positive control group (APP/PS1 mice received 2 mg/kg/d donepezil hydrochloride), high LGZG group (APP/PS1 mice received 7 g/kg/d LGZG), medium LGZG group (APP/PS1 mice received 3.5 g/kg/d LGZG) and low LGZG group (APP/PS1 mice received 1.75 g/kg/d LGZG). Mice were orally dosed with the corresponding dose of drugs every day for 4 weeks. After the test of learning and memory, a mixture of ketamine (150 mg/kg) and acepromazine (15 mg/kg) was injected intraperitoneally. The heart was transcardially perfused with normal saline. The hippocampus of the mice was then detached from surgery and preserved in liquid nitrogen. The tissues were immediately frozen at -80°C until subsequent extraction. All animal experiments were approved by the Experimental Animal Ethics Committee, Nanjing University of Traditional Chinese Medicine ahead of conducting ahead of conducting.

2.3. Morris water maze test

The white circular pool (60 cm high and 150 cm in diameter) was designed with indicators for spatial orientation and was filled with titanium white water in constant temperature (22 ± 1) °C during the whole water maze test. There was an escape platform (8 cm in diameter) 1 cm below the water maze. In the one-day spatial acquisition phase, the mice learned to find the escape platform with the help of indicators. Based on that, the mice had four trials per day in the four-day space navigation phase. The escape latency in the south-east quadrant and the distance to cross the platform were recorded by person who was blind to the grouping information. If the mice spent over 90 s to get the right way, the escape latency was recorded as 90 s.

2.4. Nissl staining

The frozen hippocampal tissue of each mouse was removed from -80°C and immersion fixed with 10% neutral formalin for 26 h, and then dehydrated and embedded in paraffin. Following deparaffinization and rehydration, the hippocampal tissue was cut into 5-μm thickness slices by the vibratome and baked at 62℃ for 45 min. All slices were dewaxed by ethanol gradients and were rinsed with distilled water. The slices were nucleated by Nissl staining solution for 5 min then rinsed with double distilled water. The slices were incubated in xylene for 12 min and then sealed with neutral gum and observed under a microscope (A1; Nikon) in multiple fields.

2.5. Perls' iron staining

The hippocampal slices as previously mentioned were treated with xylene I and II for 20 min, followed by hydrating with series of alcohol for approximately 1 min each solution. The hippocampal slices were immersed in Perls' solution (Solarbio, China) at 20-30°C for 30 min, then rinsed in double distilled water and stayed in water for 15 min. The slices were nucleated by Perls' stain reagent with 3,3'-diaminobenzidine (DAB) for 5 min, and was rinsed with distilled water for 1 min. The slices were sealed with neutral gum and photographed under a microscope (A1; Nikon) in multiple fields.

2.6. Immunofluorescence of hippocampal tissue

The hippocampal slices as previously mentioned were carefully rinsed with series of increasing concentrations of sucrose in 0.01 mol/L PBS solution. The hippocampal slices were continued to be cut into 20 μm thickness slices by the freezing vibratome. The slices were incubated with primary antibodies at 4°C for 8 h as mouse anti-human Glutathione Peroxidase 4 (GPX4) IgG (Abcam) 1:300, Neuronal nuclei antigen (NeuN) XP® Rabbit mAb (Cell Signaling) 1:500. The unbound primary antibodies were rinsed away by PBS solution. FITC-conjugated secondary antibodies (1:200) were incubated with the slices at 4°C for 8 h. The slices were stained with DAPI and the immunofluorescence images were photographed under a confocal microscope (Nikon).

2.7. Biochemical testing of Malondialdehyde (MDA) and Fe^{2+}

A portion of hippocampal tissue of each mouse was removed from -80°C and immediately cut off using razor blade in dry ice. The hippocampal tissue homogenate was lysed by RMSF and RIPA after weighing, and its cell lysate was obtained by centrifuging at 4°C at 13000 rpm for approximately 15 min. The activity of MDA in the fresh hippocampus lysate was analyzed by commercially available (Thiobarbituric Acid, TBA) assay kit (Nanjing Jiancheng, China). The MDA result was measured by the microplate reader (Bio-Rad) at 532 nm. The level of Fe^{2+} in the fresh hippocampus lysate was measured by cell ferrous iron colorimetric assay kit (Elabscenice, China) and was analyzed by the microplate reader (Bio-Rad) at 593 nm.

2.8. Determination of Glutathione (GSH)

Hippocampal tissue homogenate was weighed and

mixed with 9 times (w/w) of normal saline. GSH in hippocampal tissues of the mice was measured by microplate method assay kit (Nanjing Jiancheng, China). Hippocampal tissues were incubated with dithio bisnitrobenzoic acid (DTNB) and NADPH for 5 min. The reaction product was analyzed by the microplate reader (Bio-Rad) at 405 nm compared to reference standard.

2.9. Western blot

The hippocampal tissue homogenate was lysed by RMSF and RIPA after weighing, and its cell lysate was centrifuged at 4°C at 15000 rpm for approximately 15 min. The protein concentration was measured using the BCA kit (Beyotime). 10% SDS-PAGE was used to separate about 25 μg protein. The electrophoretic bands were transferred to PVDF membranes (Membrane-solutions). The membrane was incubated overnight at 4°C with primary antibodies as mouse anti-human NeuN IgG, AMPK, p53, solsolic vector family 7 member 11(SLC7A11), GPX4, and GAPDH (1:1000, Cell Signaling Technologies). Then, the membrane was incubated with HRP-conjugated goat anti-rabbit IgG F(ab′)2 antibody (1:5000) for 2 h at 25°C. The electrophoretic bands were stained with enhanced luminol Reagent and oxidized for 2 min and recorded by Chemi-Doc™ XRS+ imaging system (Bio-rad).

2.10. Statistical analysis

GraphPad Prism 8.0 software was applied to analyze the results. Comparisons between two groups were carried out by the unpair t-test, and comparisons between multiple groups were carried out by one-way ANOVA. A two-sided *p*-value of less than 0.05 was considered statistically significant.

3. Results

3.1. Gene set enrichment analysis

We found that the AD drug target MAPK3 was closely related to AMPK pathway and ferroptosis pathway (Fig. 1A), and MAPK3 pathway had potential regulatory relationships with ferroptosis-related genes such as SLC40A1, NCOA4, TFRC, ACSL4 and GPX4 (Fig. 1B).

3.2. LGZG promoted the spatial memory function of AD model in water maze test

LGZG exerted a significant effect on symptomatic improvement of AD, the typical behavioral traces on the 4th day of test in the water maze test were shown in Figure 2A. We confirmed AD modelling was successful by observing the escape latency of APP/PS1 model group protracted compared to the normal mice on the 4th day of space navigation trial (P<0.001), and the escape latency of positive control declined compared to the model mice (P<0.001). To assess whether LGZG had any therapeutic effect on Alzheimer's disease, high LGZG group (P<0.001) and medium LGZG group (P<0.01) appeared to progressively decline compared to the model mice as trial went on. The decline degree was dose-dependent, the more LGZG administrated, the less escape latency mice could take (Fig. 2B). Next, the positive control group (P<0.001), high LGZG group (P<0.001) and medium LGZG group (P<0.001) had a shorter path length before escaping onto the platform on the 3rd and 4th day compared to the APP/PS1 model mice (Fig. 2C), and the shorten degree also depended on the LGZG dose.

3.3. LGZG restores morphological anomalies and alleviates iron deposition

To investigate the effect of LGZG on the morphology and change of neurons number in the hippocampus of AD model, Nissl staining was performed for each group of mice. The typical Nissl-staining photos are shown in Figure 3A, we could see the morphology of the Nissl-stained tissues were abnormal in the AD model group, posi-

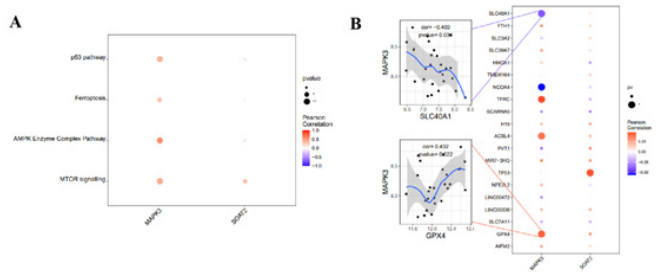

Fig. 1. Gene set enrichment analysis. (A) ssGSEA prediction of the relationship between AMPK pathway and MAPK3. (B) ssGSEA prediction of the relationship between MAPK3 pathway and ferroptosis related genes SLC40A1, NCOA4, TFRC, ACSL4, GPX4. **P<0.001.

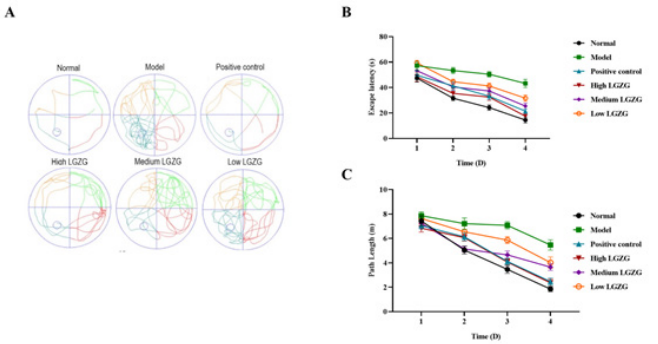

Fig. 2. LGZG promoted the spatial memory function of AD model in water maze test. (A) Typical behavioral traces of six groups mice in the water maze test. The more lines in the quadrants, the longer the escape latency. (B) The escape latency in the south-east quadrant of six groups mice. (C) The path length to cross the platform of six groups mice.

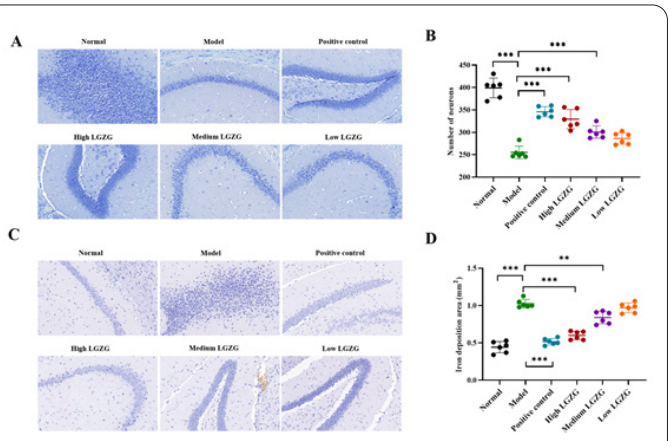

Fig. 3. LGZG restores morphological anomalies and alleviates iron deposition. (A) Typical photos of Nissl staining of six groups. (B) Nissl staining results of the number of neurons in six groups. (C) Typical photos of Perls' iron staining of six groups. (D) Perls' iron staining results of the iron deposition area of six groups. ***P<0.001.

tive control and three LGZG groups in varying degrees. There were significantly higher numbers of neurons in the normal group (P<0.001) and positive control group (P<0.001) than in the AD model group for the same area photographed. Compared to AD model group, both high LGZG(P<0.001) and medium LGZG (P<0.001) treatments elevate the number of neurons (Fig.3B), and hippocampal cells in high LGZG and medium LGZG groups were more closely arranged, the stain becomes deeper to make the vision field clearer (Fig.3A).

The Perls' iron staining results (Fig.3C) indicated that compared with the normal group, the area of iron-stained positive areas in the model group was significantly increased (P<0. 001). In contrast, the area of iron-stained positive areas of positive control group (P<0. 001) decreased compared to model group. The area of iron-stained positive areas of high LGZG group (P<0. 001) and medium LGZG group (P<0. 01) decreased as LGZG in dose-dependent manner (Fig. 3D).

3.4. LGZG alleviated oxidative stress and ferroptosis in the hippocampus of AD model

Afterwards we explored the effects of LGZG on MDA, Fe^{2+}, GSH and GXP4 in the hippocampus of AD model. The MDA contents of AD model increased abnormally compared to the normal mice (P<0.001), while the MDA levels were confirmed to decline in positive control group (P<0.001), high LGZG group (P<0.001) and medium LGZG group (P<0.01) compared to un-treated APP/PS1 model mice. The higher dose of LGZG the mice received, the more intensive effects on those levels of MDA (Fig. 4A).

The colorimetric assay showed that GSH levels decreased abnormally compared to the normal mice (P<0.001), whereas positive control group could increase the GSH levels compared to un-treated AD model (P<0.001). High dose of LGZG (P<0.001), medium dose of LGZG (P<0.01) and low dose of LGZG (P<0.01) could also rise the GSH levels compared to AD model as expected (Fig. 4B). Besides, AD model resulted in increasing of Fe^{2+} levels (P<0.001), while donepezil (P<0.001), high dose of LGZG (P<0.001), medium dose of LGZG (P<0.001) and low dose of LGZG (P<0.001) could swift to decrease the Fe^{2+} levels (Fig. 4C). The immunofluorescence assay result showed that the number of $NeuN^+$/$GPX4^+$ cells in the hippocampus of APP/PS1 model group was significantly lower than that of the normal mice (P<0.001), while the numbers of $NeuN^+$/$GPX4^+$ cells were confirmed to recover in positive control group (P<0.001), high LGZG group (P<0.001), medium LGZG group (P<0.001) and low LGZG group (P<0.001) compared to un-treated APP/PS1 model mice (Fig. 4D & 4E). According to these results, LGZG may play a key role in inhibiting lipid peroxidation and alleviating ferroptosis caused by AD *in vivo*. The number of $NeuN^+$/$GPX4^+$ cells in the hippocampus of APP/PS1 model group was significantly lower than that of the normal mice (P<0.001). LGZG restore the level of GPX4 in the hippocampus of AD model (Fig. 4F). The higher dose of LGZG the mice received, the more intensive effects on those levels of Fe^{2+}, GSH and GXP4.

3.5. LGZG protected neurofunction in AD model via AMPK pathway

Afterwards we conducted western blot to explore if LGZG regulated the protein level of NeuN, AMPK, p53, SLC7A11 and GPX4 in the hippocampus of AD model, which were all proteins related to AMPK pathway (Fig. 5A). AMPK rise in AD model compared to the normal mice. Positive control, high dose and medium dose of LGZG could reduce AMPK compared to un-treated AD model (Fig. 5B). The expression levels of NeuN in AD model decreased compared to the normal mice, whereas positive control group, high dose of LGZG and medium dose of LGZG reversed this change, restoring the expression of NeuN compared to un-treated AD model (Fig. 5C). The SLC7A11 and GPX4 levels of AD model both declined in un-treated AD model, in contrast, the SLC7A11 levels of positive control group, high dose, medium dose, and low dose of LGZG groups increased as expected (Fig. 5D, 5E). P53 rise in AD model compared to the normal mice, positive control, high dose and medium dose of LGZG could normalize p53 content compared to un-treated AD model (Fig. 5F). The higher dose of LGZG the

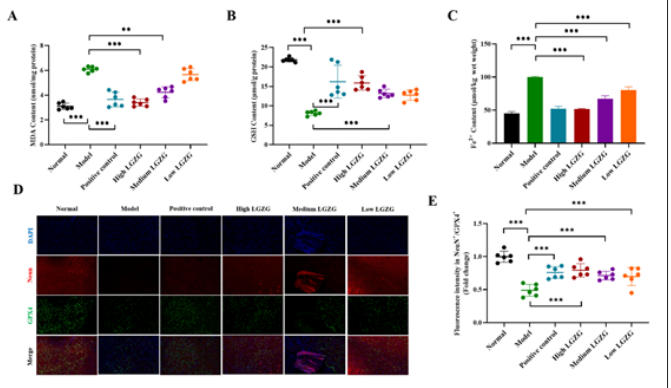

Fig. 4. LGZG alleviated oxidative stress and ferroptosis in the hippocampus of AD model. (A) The biochemical testing results for MDA of six groups. (B) The microplate assay results for GSH of six groups. (C) The biochemical testing results for Fe^{2+} of six groups. (D) Typical photos of immunofluorescence of six groups. (E) The immunofluorescence results of fluorescence intensity in $NeuN^+$/$GPX4^+$ tissues of six groups. ***P<0.001.

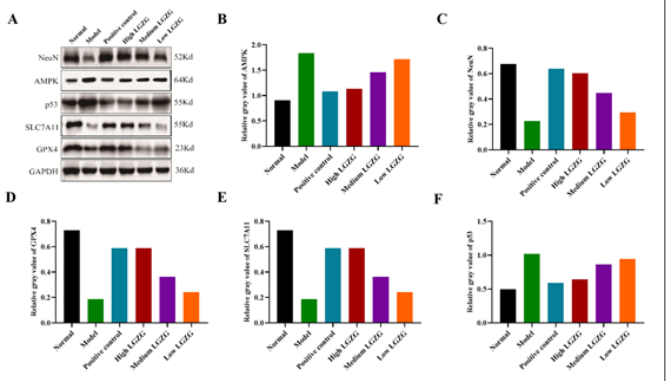

Fig. 5. LGZG protected neurofunction in AD model via AMPK pathway. Western blot photos of protein related to AMPK pathway. (B) Western blot result of relative gray value of AMPK. **P<0.01. (C) Western blot result of relative gray value of NeuN. (D) Western blot result of relative gray value of GPX4. (E) Western blot result of relative gray value of SLC7A11. (F) Western blot result of relative gray value of p53.

mice received, the more intensive effects on those protein levels in the hippocampus of AD model.

4. Discussion

Population aging and AD become cosmopolitan concerns to shake social and economic sustainability [11]. The incidence of AD reached at least 46.8 million globally in 2015, and it is expected to exceed 1.315 billion by 2050 worldwide unfortunately [12]. Despite the breaking-through progress in clinical technology of nervous system, AD is still associated with poor diagnosis and prognosis among aging society worldwide. Due to the unresolved pathogenesis conundrum and insufficient intervening measures for AD, novel tactics and better understanding of AD are in urgent need.

LGZG is a classic ancient prescription commonly used in China and Japan, which contains over 100 components, including amino acids, carbohydrates, organic acids, flavonoids, saponins, and others [13]. Modern medicine believes that the pharmacological effects of LGZG include anti-inflammatory, promoting renal function, analgesia and eliminating phlegm [14]. Rising research has indicated that those effects are associated with the treatment of inflammatory processes in cerebral disease in Chinese clinical practice [15], which inspires us to study the relationship between LGZG and AD treatment. To date, it is regrettable that there is limited literature focusing on LGZG's intervention of AD and its mechanism.

We study the role of LGZG on AD based on the classic APP/PS1 double-transgenic mouse model. APP/PS1 model imitates the neurotic plaques and neurofibrillary tangles in AD patients' brains [16]. We compared the spatial memory function and levels of AD-related molecules in both APP/PS1 model and normal mice, and set a prescription drug donepezil as positive treatment to verify the applicability of AD model. The results all indicated that APP/PS1 model was suitable for our study. The hippocampus takes major responsibility for memory and learning, especially short-term memory, which is one of the most vulnerable regions in AD patients' brains [17]. So, we took hippocampus tissues to analyze AD-related molecules and observed the morphological anomalies changes.

Learning, memory and spatial recognition ability are the most fundamental factors of AD [18]. We orally administrated three different doses of LGZG to APP/PS1 models for 4 weeks and compared the memory and spatial function by water maze test, and the LGZG's ability to improve learning function was positive relative to the LGZG dose, illustrating that LGZG was capable to improve the spatial memory function. Behavioral experiments showed that this formula was effective in AD *in vivo*. Nissl-staining results showed there were significantly higher numbers of neurons in the high and medium LGZG group, and the neurons were arranged more closely in order with deeper staining. The Nissl-stain test indicated LGZG restored morphological anomalies in the hippocampus caused by Alzheimer's disease.

Alzheimer's disease has been reported to be associated with energy transfer deficiency and oxidative stress [19]. Lipoperoxidation, resulting from abnormal intracellular oxidative stress, is regarded as the third earmark of AD tissues [20]. MDA is regarded as an important marker to reflect lipoperoxidation intensity in the central system [21]. The level of MDA could potentially indicate AD development based on the negative relationship with the MMSE testing. Our study illustrated that LGZG was helpful for AD in vivo by reducing MDA in the hippocampus, and the effect was in dose-dependent manner.

Redox-active metal ions are deeply involved in neurodegenerative disorders by O_2 transport, energy generation and oxidative stress [22]. Upregulation of Fe^{2+} has been identified to promote ferroptosis and colocalize with Aβ plaque accumulation in AD patients, which increases oxidative neurological disorders [23]. We verified that Fe^{2+} was up-regulated in APP/PS1 mice, and LGZG could inversely suppress Fe^{2+} level associated with the dose of LGZG. The Perls' iron staining results indicate that LGZG alleviated iron deposition in the hippocampus of AD model. We speculated that LGZG was able to improve symptoms and then regulate ferroptosis of neurons after spinal cord injury.

GPX4, a membrane-associated selenoenzyme, is revealed to be the major neuro protector against ferroptosis in a glutathione-dependent way [24]. GPX4 can inhibit the production of lipid peroxides during Aβ plaques accumulation in AD patients. Otherwise, lipid peroxides dissociate into hydroxy fatty acids or MDA. Our study conducted immunofluorescence and western blot to prove that LGZG could restore the level of GPX4 in the hippocampus of AD model, which may inhibit lipid peroxidation and ferroptosis in AD tissues. Collectively, the results described here strongly support that LGZG is a potential drug for neuroprotection in AD, offering a better understanding of LGZG and the pathogenesis mechanisms responsible for AD.

Then we focused on how LGZG inhibited AD progress. Rising research has indicated that AMPK pathway deregulation plays a critical role in multiple neurodegenerative diseases, such as Alzheimer's disease, Parkinson's disease and Huntington's disease. Abnormal AMPK signaling underlies the damage to synaptic plasticity associated with Alzheimer's disease, making it a potential therapeutic mechanism for Alzheimer's disease [25]. SsGSEA algorithm forecasted that AMPK pathway was indeed dysfunctional in AD, and AMPK pathway and ferroptosis pathway had strong band with the drug target MAPK3 of AD. Our study proved that LGZG normalized the protein level of NeuN, AMPK, p53, SLC7A11 and GPX4 in the hippocampus of AD model. LGZG modifies the content of many proteins related to intracellular AMPK signaling, suggesting that AMPK may play an important role in the regulation of AD progression, but the specific mechanism still needs to be further verified.

5. Conclusion

In summary, our study has confirmed that this formula LGZG has a protective effect on AD, it is a viable strategy to explore in the treatment of AD. To date, our understanding of the mechanisms of LGZG driving AD mitigation is limited. The major insufficiency is that we only explore the effects of LGZG on one AD mouse model. The molecule mechanisms of LGZGs to interact with AMPK pathway and other regulators will be our further research direction, such as AMPK-related protein phosphorylation or combination.

Conflict of interests

The authors declare no competing interests.

Consent for publications
The author read and approved the final manuscript for publication.

Ethics approval and consent to participate
We have received approval from the Experimental Animal Ethics Committee of Nanjing University of Traditional Chinese Medicine.

Informed consent
Not applicable.

Availability of data and material
The data that support the findings of this study are available from the corresponding author upon reasonable request.

Authors' contributions
ZC contributed to the study conception and design. Experimental operation, data collection and analysis were performed by FY, LY, HJ and HZ. The first draft of the manuscript was written by FY and all authors commented on previous versions of the manuscript.

Funding
Not applicable.

Acknowledgements
Not applicable.

References

1. Javaid SF, Giebel C, Khan MA, Hashim MJ (2021) Epidemiology of Alzheimer's disease and other dementias: rising global burden and forecasted trends. F1000 Research 10: 425.
2. Tahami Monfared AA, Byrnes MJ, White LA, Zhang Q (2022) Alzheimer's Disease: Epidemiology and Clinical Progression. Neurol Ther 11 (2): 553-569. doi: 10.1007/s40120-022-00338-8
3. Talmelli LF, Gratão AC, Kusumota L, Rodrigues RA (2010) Functional independence level and cognitive deficit in elderly individuals with Alzheimer's disease. Rev Esc Enferm USP 44 (4): 933-939. doi: 10.1590/s0080-62342010000400011
4. Liu L, Zhao Y, Birling Y, Sun Y, Shang Q, Hu ZJ, Liu J, Liu Z (2022) Effectiveness and safety of Linggui Zhugan decoction for the treatment of premature contraction in patients with coronary heart disease: A systematic review and meta-analysis. Front Cardiovasc Med 9: 1002378. doi: 10.3389/fcvm.2022.1002378
5. Chen DS, Ke B, Huang YJ, Meng J, Zhang JJ, Chen ZX, Michalsen A, Qin J (2011) Effects of the modified linggui zhugan decoction (see text) combined with short-term very low calorie diets on glycemic control in newly diagnosed type 2 diabetics. J Tradit Chin Med 31 (3): 185-188. doi: 10.1016/s0254-6272(11)60038-1
6. Liu T, Yang LL, Zou L, Li DF, Wen HZ, Zheng PY, Xing LJ, Song HY, Tang XD, Ji G (2013) Chinese medicine formula lingguizhugan decoction improves Beta-oxidation and metabolism of Fatty Acid in high-fat-diet-induced rat model of Fatty liver disease. Evid Based Complement Alternat Med 2013: 429738. doi: 10.1155/2013/429738
7. Han J, Zhang H, Zhang Y, Zhang Z, Yu M, Wang S, Han F (2022) Lingguizhugan decoction protects PC12 cells against Aβ(25-35)-induced oxidative stress and neuroinflammation by modulating NF-κB/MAPK signaling pathways. J Ethnopharmacol 292: 115194. doi: 10.1016/j.jep.2022.115194
8. Zhu M, Hao S, Liu T, Yang L, Zheng P, Zhang L, Ji G (2017) Lingguizhugan decoction improves non-alcoholic fatty liver disease by altering insulin resistance and lipid metabolism related genes: a whole trancriptome study by RNA-Seq. Oncotarget 8 (47): 82621-82631. doi: 10.18632/oncotarget.19734
9. Xu W, Luo Y, Yin J, Huang M, Luo F (2023) Targeting AMPK signaling by polyphenols: a novel strategy for tackling aging. Food Funct 14 (1): 56-73. doi: 10.1039/d2fo02688k
10. Liu YJ, Chern Y (2015) AMPK-mediated regulation of neuronal metabolism and function in brain diseases. J Neurogenet 29 (2-3): 50-58. doi: 10.3109/01677063.2015.1067203
11. Brivio P, Paladini MS, Racagni G, Riva MA, Calabrese F, Molteni R (2019) From Healthy Aging to Frailty: In Search of the Underlying Mechanisms. Curr Med Chem 26 (20): 3685-3701. doi: 10.2174/0929867326666190717152739
12. Passeri E, Elkhoury K, Morsink M, Broersen K, Linder M, Tamayol A, Malaplate C, Yen FT, Arab-Tehrany E (2022) Alzheimer's Disease: Treatment Strategies and Their Limitations. Int J Mol Sci 23 (22). doi: 10.3390/ijms232213954
13. Li B, Fan S, Hu J, Ma Y, Feng Y, Wang F, Wang X, Niu L (2021) Phytochemical Analysis Using UPLC-MS/MS Combined with Network Pharmacology Methods to Explore the Biomarkers for the Quality Control of Lingguizhugan Decoction. Evid Based Complement Alternat Med 2021: 7849032. doi: 10.1155/2021/7849032
14. Xi F, Sang F, Zhou C, Ling Y (2012) Protective effects of Lingguizhugan decoction on amyloid-beta peptide (25-35)-induced cell injury: Anti-inflammatory effects. Neural Regen Res 7 (36): 2867-2873. doi: 10.3969/j.issn.1673-5374.2012.36.003
15. Xue TC, Ge NL, Zhang L, Cui JF, Chen RX, You Y, Ye SL, Ren ZG (2014) Goosecoid promotes the metastasis of hepatocellular carcinoma by modulating the epithelial-mesenchymal transition. PLoS One 9 (10): e109695. doi: 10.1371/journal.pone.0109695
16. Stalder M, Deller T, Staufenbiel M, Jucker M (2001) 3D-Reconstruction of microglia and amyloid in APP23 transgenic mice: no evidence of intracellular amyloid. Neurobiol Aging 22 (3): 427-434. doi: 10.1016/s0197-4580(01)00209-3
17. Rao YL, Ganaraja B, Murlimanju BV, Joy T, Krishnamurthy A, Agrawal A (2022) Hippocampus and its involvement in Alzheimer's disease: a review. 3 Biotech 12 (2): 55. doi: 10.1007/s13205-022-03123-4
18. Cherrier MM, Mendez M, Perryman K (2001) Route learning performance in Alzheimer disease patients. Neuropsychiatry Neuropsychol Behav Neurol 14 (3): 159-168.
19. Atamna H, Frey WH, 2nd (2007) Mechanisms of mitochondrial dysfunction and energy deficiency in Alzheimer's disease. Mitochondrion 7 (5): 297-310. doi: 10.1016/j.mito.2007.06.001
20. Foley P (2010) Lipids in Alzheimer's disease: A century-old story. Biochim Biophys Acta 1801 (8): 750-753. doi: 10.1016/j.bbalip.2010.05.004
21. de Farias CC, Maes M, Bonifácio KL, Bortolasci CC, de Souza Nogueira A, Brinholi FF, Matsumoto AK, do Nascimento MA, de Melo LB, Nixdorf SL, Lavado EL, Moreira EG, Barbosa DS (2016) Highly specific changes in antioxidant levels and lipid peroxidation in Parkinson's disease and its progression: Disease and staging biomarkers and new drug targets. Neurosci Lett 617: 66-71. doi: 10.1016/j.neulet.2016.02.011
22. Kim N, Lee HJ (2021) Redox-Active Metal Ions and Amyloid-Degrading Enzymes in Alzheimer's Disease. Int J Mol Sci 22 (14). doi: 10.3390/ijms22147697
23. Wu Y, Torabi SF, Lake RJ, Hong S, Yu Z, Wu P, Yang Z, Nelson K, Guo W, Pawel GT, Van Stappen J, Shao X, Mirica LM, Lu Y (2023) Simultaneous Fe(2+)/Fe(3+) imaging shows Fe(3+) over Fe(2+) enrichment in Alzheimer's disease mouse brain. Sci Adv 9 (16): eade7622. doi: 10.1126/sciadv.ade7622
24. Lane DJR, Metselaar B, Greenough M, Bush AI, Ayton SJ (2021) Ferroptosis and NRF2: an emerging battlefield in the neurodege-

neration of Alzheimer's disease. Essays Biochem 65 (7): 925-940. doi: 10.1042/ebc20210017

25. Chen M, Huang N, Liu J, Huang J, Shi J, Jin F (2021) AMPK: A bridge between diabetes mellitus and Alzheimer's disease. Behav Brain Res 400: 113043. doi: 10.1016/j.bbr.2020.113043